WBL DETONATION WAVE PROPAGATION FOR EDC35 AND EDC37

A.M.Collyer, J.D.Dunnett, D.C.Swift*, and S.J.White
AWE, Hydrodynamics Department, Aldermaston, Reading, RG7 4PR, United Kingdom

The WBL (Witham – Bdzil – Lambourn) detonation model[1,2,3] is a computationally efficient way of predicting the motion of a detonation wave in explosives without the need to resolve the reaction zone in a continuum mechanics calculation. Level set methods have been employed to model experiments, where they have been found to be more convenient than schemes which move the detonation wave as an explicitly represented surface. Measurements have been made of the angle which detonation waves in EDC37 make with inert materials. These angles are required as boundary conditions for the WBL model and to test theoretical models of the structure of the reaction zone. Experiments of different sizes have been fired using EDC37 and the insensitive high explosive EDC35, with measurements of the shape of the detonation wave at the end of each charge, allowing relations between the speed and curvature of the detonation wave to be found in each explosive.

INTRODUCTION

Models such as the WBL act as a bridge between Chapman-Jouguet detonation and reactive flow calculations. They allow some non-ideal behaviour without requiring a finely resolved treatment incorporating explosive reaction. Considered as an iterative improvement, they posses fewer free parameters than a full reactive flow model and hence can be characterised by fewer experimental measurements. The WBL model is effectively a correction to the Huygen's wave propagation method often used in hydrocodes.

A new analytic method for calculating detonation wave propagation with the WBL model is presented. This is based on field evolution of the burn characteristics of the explosive, allowing more versatile modelling of complex shapes and burn mechanisms.

To corroborate the WBL model further, experiments have been fielded to find data for the model. These involved cylinders and slabs of the TATB-based insensitive high explosive (IHE) EDC35 and HMX-based EDC37, together with boundary angle trials on EDC37. The results of these experiments are presented.

WBL DETONATION

The WBL model describes the propagation of the leading shock of a detonation wave. The local speed, D, at which any portion of the wave propagates along its normal direction, is a function of its geometry, in particular the local mean wave curvature K. A key piece of information required to characterise the detonation behaviour of an explosive is the $D(K)$ relation.

Inert materials exert a 'dragging' effect on the detonation wave. This is described by prescribing a preferred angle, φ_a, which the wave makes with inert materials. It is postulated that this angle can be predicted, given an understanding of certain explosive and inert properties, or measured directly from wave shape experiments. An additional boundary condition is the angle φ_c at which a detonation wave (meeting an inert boundary from an initially low angle of incidence) can first be influenced by the boundary – the causal angle.

'LEVEL-SET' TECHNIQUES FOR PROPAGATING DETONATION WAVES

The propagation of waves as described by the WBL model may be computed using a *wave-tracking* approach, i.e. approximating the wave as a finite set of Lagrangian marker particles whose subsequent movement are governed by the WBL equations of motion. This technique has been seen to be accurate and efficient for simple problems such as single waves propagating through slabs or cylinders of high explosive. In general, however, this solution method did not readily extend to handle increasing complex problems. In particular, extensive additional coding was required to locate and handle wave collisions, complicated charge boundary interactions and corner turning.

'Level-set' methods[4], or Propagation of Surfaces under Curvature (PSC), offer an alternative approach for calculating wave propagation – one which extends easily to accommodate those more convoluted modelling problems mentioned above. This technique determines wave motion by relating the wave front to an isosurface, $\psi(\underline{r},t) = C$, of some evolving scalar function, ψ, defined over all space, $\underline{r}$, and time, t.

* now with Fluid Gravity Engineering / Edinburgh University

In order for a wave front, propagating with curvature dependent speed $D(K)$[4,5], to remain coincident with a defined isosurface, the field must evolve according to the equation:

$$\frac{\partial \psi}{\partial t} - D(K)\left|\nabla \psi\right| = 0 \qquad (1)$$

Curvature may be computed from the divergence of the wave outward normals as follows:

$$K = \frac{(\nabla \cdot \underline{n})}{2} \qquad (2)$$

In our work, the wave front is taken to be the $\psi=0$ isosurface, with $\psi>0$ in the burnt explosive region behind the wave and $\psi<0$ in the still unburned explosive. The wave normal is thus obtained from

$$\underline{n} = -\frac{\nabla \psi}{\left|\nabla \psi\right|} \qquad (3)$$

First generation 2D and 3D schemes were devised which predict wave propagation by calculating the evolution of a field specified on a Cartesian mesh. In these implementations, the field values, ψ, were defined at node points with the vectors $\nabla\psi$ and $\underline{n}$ computed at cell centres. Time integration was performed using a forward time upwinding scheme.

Cells through which the charge boundary passes are defined as boundary cells; each boundary cell has an associated vector defining the charge surface outward normal. User defined boundary conditions are applied in these cells by rotating $\underline{n}$ until it is consistent with the prescribed values of φ_A and φ_C.

These initial implementations demonstrated the viability of the method and underlined two of its major strengths: the implicit handling of multiple wave collisions and the ease with which the method extends from two to three dimensions. Nevertheless, the Cartesian approach had shortcomings: curved and irregular shaped charge boundaries could only be represented approximately and computational effort was often wasted computing field evolution in external inert regions.

A subsequent second generation of schemes generalised the algorithms to allow wave propagation to be computed on arbitrary meshes - in particular, meshes which exactly fitted the explosive's form. In these schemes, the discretisation was reversed: the ψ field was defined at the cell centres and $\nabla\psi$ computed at (internal) node points by fitting planes (hyper-planes in 3D) to the surrounding ψ values. A predictor-corrector scheme was used for the time integration to give increased accuracy.

$\nabla\psi$ was evaluated at boundary (exterior) nodes by simply copying the vector from a designated 'nearest interior node'. Boundary conditions were applied as in the Cartesian schemes simply by rotating the wave normal, $\underline{n}$, so as to achieve consistency with the supplied values of φ_A and φ_C again.

The rotation of the wave normals at the boundary results in an increase in curvature and subsequent decrease in wave speed - the boundary effectively exerts a 'drag' on the wave. An example of this is seen in Figure 1 which shows wave shapes taken at 0.2μs intervals from a calculation (performed using the 2D arbitrary mesh scheme) of an initially planar wave propagating along a cylinder of explosive.

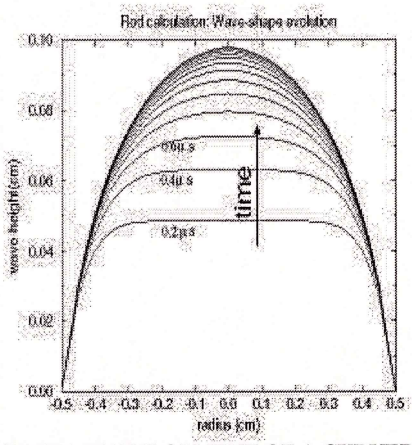

FIGURE 1. DEVELOPMENT OF A CURVED WAVE FRONT FROM A PLANE INITIATION USING LEVEL SET (PSC) METHODS

A linear $D(K)$ relation was used:

$$D = D_{cj}(1 - AK) \qquad (4)$$

where D_{cj} and A were taken to be 7.818mm/μs and 0.5mm respectively. Boundary angles of $\varphi_A=\varphi_C=49.9°$ were applied as constraints along the rod's surface. As is seen, the effect of the drag at the boundary propagates inward and the initially flat wave becomes increasingly curved as it assumes a steady shape.

It can be shown that for a wave propagating subject to a linear $D(K)$ relation along a cylinder of explosive of radius

R, the steady state (in terms of diffusion) wave shape is well approximated by the following ratio of zeroth-order Bessel functions:

$$z(r) = a \ln\left(\frac{J_0(br)}{J_0(bR)}\right) \tag{5}$$

where

$$a = \frac{A}{3-2l}, \quad b = \frac{\sqrt{2(1-l)(3-2l)}}{A}, \quad l = \frac{D0}{Dcj} \tag{6}$$

and where $D0$ is the phase speed of the wave and is dependent on the applied boundary constraints. Applying Equation 5 to a 5mm radius cylinder problem, we found that the φa=φc=49.9° boundary conditions corresponded to a phase speed of 7.643mm/μs. This compares well with a steady wave phase speed of 7.645mm/μs observed in the calculation.

The success of the calculation – and the general suitability of the technique – is further demonstrated by the close match between the calculated steady wave shape and the shape given by Equation 5, as seen in Figure 2. A comparison with EDC37 can be seen later in the paper (Figure 10).

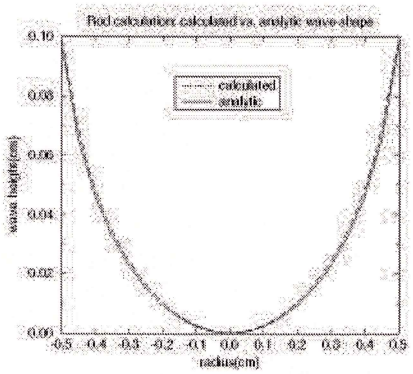

FIGURE 2. ANALYTIC SOLUTION AND LEVEL-SET PREDICTION FOR A STEADY WAVE

BOUNDARY ANGLES

It has been postulated that the 'preferred angle', φa, between a detonation wave and a high acoustic impedance (ρc) inert material is where no reflected wave (NRW) is produced at the intersection point. Predicting φa in this way requires knowledge of the equation of state of the shocked explosive, which is difficult to obtain experimentally at detonation pressures. Values for φa were predicted for detonation waves in EDC37 alongside a variety of inert materials and slab experiments fired to compare the findings.

The causal angle, φc, at which a detonation wave can first be influenced by an inert material, is approximately equal to the angle at which information at the local sound speed sweeps across the wave.

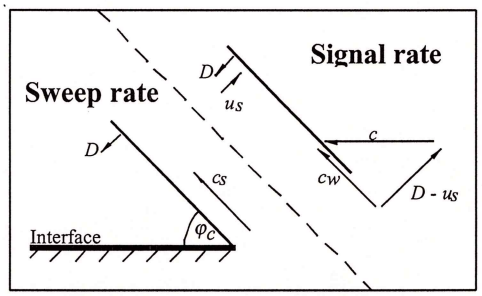

FIGURE 3. CAUSAL ANGLE CALCULATION

From Figure 3, there are two components involved in calculation of φc; the sweep rate (the rate at which the interface effectively sweeps across the wave front) and the signal rate (the rate at which information propagates across the wave at the local sound speed).

Sweep: $$cs = \frac{D}{\tan \varphi c} \tag{7}$$

Signal: $$cw = \sqrt{c^2 - (D - us)^2} \tag{8}$$

Then φc is found where cs=cw, i.e.

$$\Rightarrow \quad \varphi c = \arctan\left(\frac{D}{\sqrt{c^2 - (D-us)^2}}\right) \tag{9}$$

For low impedance materials, φc should equal φa as the interface reflects a rarefaction into the detonation products, flattening any wave with φ<φc to the point where the causal angle is reached[6].

From this it can be seen that whereas φa is dependent on the material properties of the explosive *and* inert components, φc is entirely a function of the explosive. By

applying Equation 9, φ_C for EDC37 is found to be approximately 54.2°, and for EDC35, φ_C=49.0°.

Experiments were performed to measure φ_a from the shape of a detonation wave emerging from line initiated slabs of EDC37. A typical round can be seen as Figure 4.

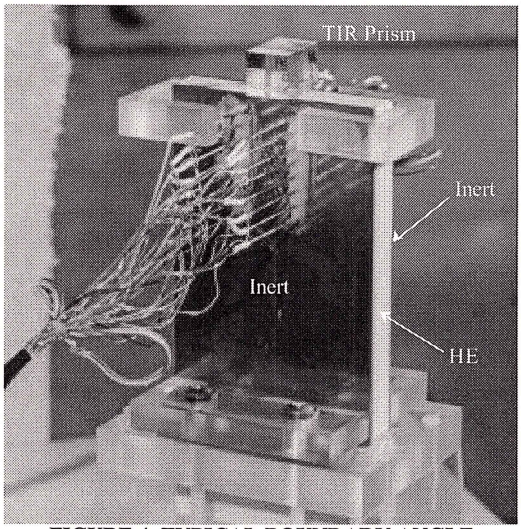

FIGURE 4. TYPICAL BOUNDARY ANGLE MEASUREMENT EXPERIMENT

120mm long x 75mm wide x 12.7mm thick slabs of EDC37 were line initiated along one short side and the resulting detonation wave emerging from the top measured by a Total Internal Reflection (TIR) technique.

The 75mm width was chosen so that the central region of explosive being measured was not perturbed by the edges in the third dimension during the 120mm run. This was considered long enough to produce a sufficiently stable wave in the region of interest, given the narrow width and the input wave meeting the inert close to the causal angle.

With the exception of ABA7, the shape of the detonation wave was recorded on a high speed electronic streak camera with a writing rate of ~100mm/μs. This seventh round was diagnosed using a rotating mirror camera, writing at ~30mm/μs.

Two plates of inert material were placed in contact with the explosive and ionisation probes allowed the phase speed ($D0$) of the wave to be found. The phase speed was measured so that the recorded temporal wave shape could be converted into a spatial shape for comparison with the analytic solution.

Eight experiments were fired in total, the first being to characterise the output from the line initiator only. Of the remaining seven experiments - with the exception of the final (corroborative) shot - all rounds had the same inert on both sides of the charge. A list of inert materials used in those seven rounds appears in Table 1.

TABLE 1. INERT MATERIALS FOR ASYMPTOTIC BOUNDARY ANGLE EXPERIMENTS

Round	Inert	Density (g/cc)
ABA1	Air	0.0
ABA2	Copper	8.9
ABA3	Aluminium	2.7
ABA4	Rubber / Aluminium†	1.66 / 2.7
ABA5	Tantalum	16.6
ABA6	Potting / Tantalum†	1.06 / 16.6
ABA7	Side I - Aluminium Side II - Copper	2.7 8.9

† The inert listed first was next to the explosive.

Using the TIR technique, light was continually reflected off the bottom surface of the prism, in contact with the explosive, until the detonation wave arrived, disrupting the total internal reflection and extinguishing the light to the camera, giving a record as seen in Figure 5.

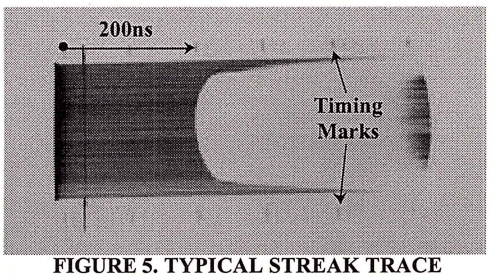

FIGURE 5. TYPICAL STREAK TRACE

To accurately characterise the camera streak rate, a pulsed laser was used to mark the film at regular (known) intervals (Figure 5).

With the streak trace digitised, a quadratic fit was applied to the spatial wave shape near each of the explosive/inert interfaces. From this, an angle between the wave front and the interface was found. When the phase speeds were measured for the two different materials in round seven, they were seen to agree with each other to 0.3%, giving confidence that the wave had stabilised.

In some cases, a bright-up was seen on the streak image at the explosive/inert interface. This was caused by a flash as air trapped between the explosive and inert was compressed. The brightness of this and the high sensitivity of the camera resulted in part of the desired image being obscured. In these cases, extrapolation was performed to obtain an edge angle. This method was not required for ABA7, which gave good agreement to earlier results obtained by wave front data extension, thus corroborating this method. The results obtained from analysis of the streak traces, are shown in Table 2. Each experiment gave two results, one from either side.

TABLE 2. BOUNDARY ANGLES FOR EDC37

Round	Angle I (°)	Angle II (°)
ABA1	40.56	49.55
ABA2	77.94	75.82
ABA3	78.79	76.99
ABA4	61.11	57.77
ABA5	68.15	69.74
ABA6	50.54	54.84
ABA7	78.61 (Al)	78.22 (Cu)

The experimental error in each edge angle was calculated from worst-case inaccuracies in the calculation of the camera writing speed, the measurement of the phase speed and the magnification of the image. The average error in the edge angle due to the three factors together was ±0.12°.

The theoretical postulates for boundary angles were put to the test for the impedance range tested in the experiments. The results, together with the empirical findings, are seen in Figure 6.

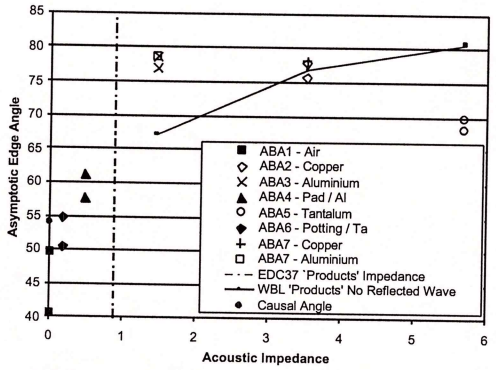

FIGURE 6. THEORY AND EXPERIMENTAL RESULTS FOR EDC37

There is a striking miscorrelation between the predicted and the experimentally observed edge angles. Whereas WBL NRW theory states that the edge angle for inerts with impedances above that of the explosive will increase monotonically with acoustic impedance (i.e. the wave will become less curved), early findings suggest a fall-off in angle.

For inerts with impedances below that of the explosive, although the trend is in the general direction of the causal angle, it does not meet the value exactly, actually ending up below it as $\rho c \rightarrow 0.0$.

One area that is to be investigated is the choice of explosive EOS to be used when calculating the NRW condition through shock refraction. Presently, a JWL products EOS has been used (Figure 6). From shock refraction, any reflected wave (if the point of interaction remains on the interface) reflects into the material *immediately* behind the shock wave. If a detonation wave is thought of as having a finite thickness, with a leading shock (LS) followed by a region of burning, to a point where a sonic surface marks the back of the reaction zone, then using a products EOS is highly simplified.

Treating the LS as a purely unreactive pressure spike, a modified JWL EOS with a parameter free extension[6], was tried to allow an unreacted state to be modelled.

$$p = f(v, e)_{JWL} - (1-\lambda)\frac{\omega}{v}(e_0 + e^*) \qquad (10)$$

where λ is the reaction fraction: 0 for unreacted and 1 for fully reacted (returning the standard JWL EOS), and

$$e^* = \frac{v_0}{\omega}\left[A\left(1-\frac{\omega}{R_1}\right)e^{-R_1} + B\left(1-\frac{\omega}{R_2}\right)e^{-R_2} - p_0\right] \qquad (11)$$

This extension is based on a constant volume reaction and an offset between the specific internal energies of the unreacted explosive and its products. Although originally designed for IHE work, it has been applied here as a first attempt at an unreacted EOS for EDC37. However, neither gave the observed trends in the data, but a better EOS and wave refraction model for the von Neumann spike may be advantageous for future analysis of the mechanisms involved.

Another issue is the definition of 'No Reflected Wave'. What is really meant in the WBL model is a steady state flow situation behind the leading shock. There could still be a steady state evident in the following flow even with a reflected wave, whereby the reflected wave has a stabilising effect on the flow immediately behind the LS.

SPEED-CURVATURE RELATIONS

A *D(K)* relation, together with a value for φa, defines the steady-state shape and speed of a detonation wave in a long cylinder or slab of explosive. Conversely, measurements of the shape and speed allow a *D(K)* relation to be deduced.

A series of rounds of different sizes have been fired for EDC35, and a unique, non-linear *D(K)* relation deduced[3]. There are some systematic residuals in the fit to the wave shapes, and work is in progress to determine whether this implies that the *D(K)* relation must be generalised to include acceleration terms, e.g. expressed as a relation $\dot{D}(D,K)$. A similar series of rounds was fired for EDC37.

The key requirement for this type of experiment is for the detonation wave to have become stable, for subsequent comparison with the analytic solution. The diameter/width of each experiment was chosen so as to be able to form a *D(K)* over a reasonable curvature range. From this, the length of the explosive needed to reach stability was calculated. A theory was formulated stating that, for a linear *D(K)* of the form in Equation 4, the length of charge, *L*, needed to ensure a steady state was calculable from the following expression:

$$L = v\frac{2d^2}{A\pi^2} + r_f \qquad (12)$$

where v is a stability factor (a dimensionless value related to the time to asymptote to a steady wave shape), d is the charge diameter/thickness, A is the linear *D(K)* parameter, and rf is a term used when the initiation is point rather than plane (because of the finite run distance for the wave to reach the boundary at the causal angle). It can be readily seen from Equation 12 that for a given value of stability factor v, the charge length increases as the square of the diameter. A value of $v>1$ is felt adequate to define a stable system.

Although past results on the HMX-based explosive EDC29[3] were of questionable stability, it gave an indication as to the required length of the EDC37 charges because of the similar detonation properties of the two explosives.

The experimental design was effectively the same in all cases. Cylinders and slabs of various lengths and diameters/thicknesses were detonated at one end and left to run to a steady state. For the EDC37 rounds, a trace of the shape could be recorded using an electronic camera by extinction of reflection of light from gold leaf on the end of the explosive as the detonation wave arrived. A typical EDC37 experiment can be seen as Figure 7.

The earlier EDC35 rounds used a self illumination technique to reveal the wave shape on a rotating mirror camera – running at approximately a third of the writing speed of the electronic camera.

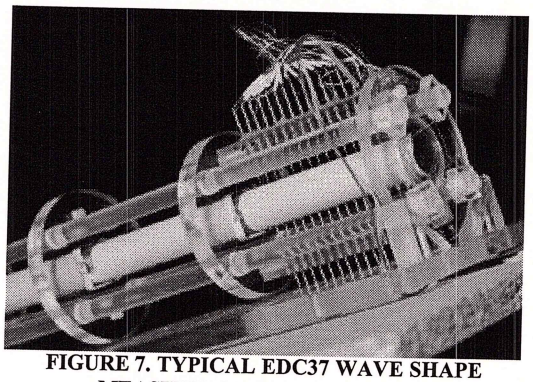

FIGURE 7. TYPICAL EDC37 WAVE SHAPE MEASUREMENT EXPERIMENT

As in the boundary angle experiments, ionisation probes were used to obtain the phase speed of the detonation wave in the last few centimetres of the run. These were placed perpendicular to the optical measurement plane to minimise any perturbing effects.

EDC35 *D(K)* RELATION

Six experiments were fielded to establish a *D(K)* fit for EDC35; a mixture of cylinders and slabs over a range of diameters/thicknesses, as seen in Table 3. As a starting point, a linear *D(K)* (Equation 4) was fitted to each experiment independently to see if there was any correlation with geometry or scale. This was achieved by applying a stable wave fitting software suite that returns values for Dcj and A after a least squares fit of the digitised experimental wave shape. The parameters obtained are also shown in Table 3.

TABLE 3: EDC35 *D(K)* DETAILS

Round	Geometry	Width (mm)	Length (mm)	Dcj (mm/μs)	A (mm)
WBL21	Cylinder	50.8	762.0	7.747	1.852
WBL15	Cylinder	10.0	60.0	7.781	0.600
WBL17	Slab	10.0	60.0	7.555	0.465
WBL18	Slab	10.0	60.0	7.614	0.604
WBL9	Slab	20.0	120.0	7.745	0.633
PS26	Slab	25.0	120.0	7.809	1.560

When plotted on *D-K* axes (Figure 8), it became evident that a single linear *D(K)* would not be sufficient to describe the complete range of curvatures observed in the various experiments. It also gave a clue as to the likely shape of a single functional fit - if one could be found - i.e. steep at low curvatures, flattening off as *K* increased.

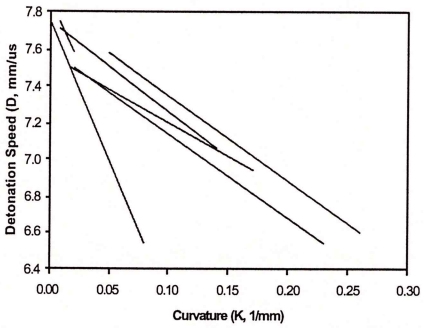

FIGURE 8. SERIES OF LINEAR *D(K)* RELATIONS FOR EDC35

A form was found for this type of behaviour from J B Bdzil's 'detonation shock dynamics' fit to PBX9502[7]:

$$D = Dcj\left\{1 + F\left[\left(\kappa_f - \kappa\right)^{\mu} - \kappa_f{}^{\mu}\right] - \frac{A^{*}\kappa^{1/\nu}}{1 + B\kappa^{\omega}}\right\} \quad (13)$$

where all parameters except D and κ are explosive dependent. It can be seen that when F=0.0, ν=1.0 and B=0.0, the linear relation is recovered with $A^{*}=A/2$. In this equation, κ is the independent variable and is connected to the WBL curvature, K, by the relation $K=\kappa/2$.

This analytic form was coupled to a Levenberg-Mardquart *n*-parameter fitting routine, using a simple numerical differentiation scheme to determine the Jacobian matrix that comes from the method. This was necessary because all the experimental data were in spatial (r,z) form whereas the fit was to (D, κ).

Along with the *(r,z)* data, diameter effect values were required. This was in the form of a table of *r,D0* data points for the rounds used. Two separate tables were required: one for the cylinders and one for the slabs. To reduce the sensitivity of the results to *D0*, a scaled average of the phase speeds was used.

A single fit to all experiments using this non-linear *D(K)* was successful, yielding the following parameters: Dcj=7.818mm/μs, F=0.207, μ=0.7896, κf=1.397mm^{-1}, A^{*}=0.3324mm, ν=1.7908, B=9.9133mm, ω=0.7574. This fit was obtained with a causal angle of 50°.

Confidence in the form of this non-linear function was gained by forming a tabular *D(K)*. This did away with any artificial constraints placed on a functional form. A linear speed-curvature relation was chosen as a starting point. Then by applying all experimental data points simultaneously and iteratively applying weighting to regions of high and low sensitivity, a table of *D(K)* points was found over the complete curvature range.

Figure 9 shows the correlation between the free-form tabular *D(K)* and the non-linear fit (Equation 13) for EDC35. (The kink in the tabular plot was always evident in the fitting routine output, thus giving the impression that it is a true reflection of the data behaviour.)

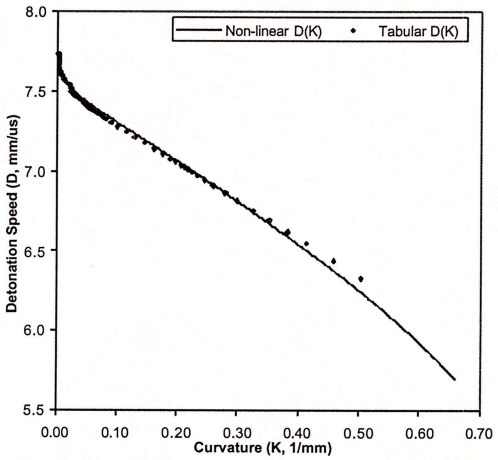

FIGURE 9. TABULAR AND NON-LINEAR *D(K)* FOR EDC35

The tabular speed-curvature relation obviously follows a similar trend to that given by the non-linear *D(K)*, although as there are no tabular (i.e. experimental) values for curvatures beyond ~0.5mm^{-1}, any *D(K)* response gained from the analytic solution in this region must be treated with caution.

EDC37 *D(K)* RELATION

Similar experiments were fielded for EDC37. To date, only cylindrical charges have been fired, as detailed in Table 4.

TABLE 4. EDC37 *D(K)* EXPERIMENT DETAIL

Round	Diameter (mm)	Length (mm)
ADK1	10.0	150.0
ADK2	10.0	300.0
ADK3	20.0	600.0
ADK4	20.0	600.0

One linear *D(K)* fit was found that matched the average of both the ADK3 & 4 wave shapes: D_{cj}=8.764mm/μs, A=0.162mm.

From a calculation using the PSC code, this *D(K)* gave a very good match for a simulation of the larger diameter experiments in terms of wave shape (Figure 10) and phase speed. The result from a standard Huygen's construction wave propagation method is also shown on the figure. This serves to highlight the difference between the basic – and often used – Huygen's method and the WBL correction when applied to EDC37 – a variation of approximately 35ns at the edge of the charge in this case.

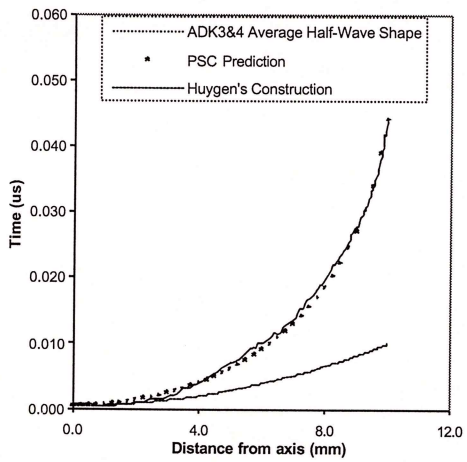

FIGURE 10. EDC37 STEADY WAVE COMPARISON

When this *D(K)* was applied to calculations of ADK1 & 2, there was a distinct difference between the predicted phase speed and that seen in the experiments. To correct this, it is necessary to have a *D(K)* of steeper gradient in this higher curvature regime; agreeing with the behaviour of the non-linear *D(K)* used so successfully for EDC35. These findings promote the idea that a non-linear form is required for HMX-based EDC37 as well as for the IHE EDC35.

To obtain a non-linear *D(K)* for EDC37 more wave shapes are required. Work is in hand to fire additional EDC37 ADK experiments, ranging from 10mm diameter x 150mm long to 30mm diameter x 1360mm long.

CONCLUSIONS AND FUTURE WORK

'Level set' methods or PSC schemes have been employed successfully to calculate the propagation of detonation waves in 2D and 3D. In 3D, their robustness and simplicity makes them preferable to wave-tracking (eikonal) methods.

Theoretical predictions and experimental measurements have been done on the angles between detonation waves in EDC37 and inert boundary materials. Preliminary results show discrepancies between theoretical and experimental findings, although more ideas have yet to be investigated. Further work into the theoretical predictions and more corroborative experiments are needed. Similar experiments on EDC35 are also planned for the future.

Non-linear speed-curvature relations have been found for EDC35, with the same form looking promising for EDC37.

REFERENCES

1. Lambourn B.D. and Swift D.C., "Application of Witham's Shock Dynamics Theory to the Propagation of Divergent Detonation Waves," Proc 9th Symposium (International) on Detonation, OCNR 113291-7, 1989.

2. Swift D.C. and Lambourn B.D., "A Review of Developments in the WBL Detonation Model," Proc 10th Symposium (International) on Detonation, ONR 33395-12, 1993.

3. Collyer A.M., Johnson A.M., Selby P.A., Swift D.C. and White S.J., "Detonation Wave Propagation in EDC35," Proc 4e Symphosium(*sic*) International Hautes Pressions Dynamiques, CEA, 1995.

4. Osher S. and Sethian J.A., "Fronts Propagating with Curvature-Dependant Speed: Algorithms Based on Hamilton-Jacobi Formulations," J. Comp. Phys., 79, 12-49, 1988.

5. Bdzil J.B. and Aslam T., Los Alamos National Laboratory, private communications, 1997.

6. Swift D.C. and White S.J., "An Evaluation of Detonation Models," Journal de Physique IV, Colloque C4, supplément au Journal de Physique III, 5, pp37-47, May 1995.

7. Bdzil J.B., "DSD Characterisation of PBX9502," Proc 10th Symposium (International) on Detonation, 1993.

DISCUSSION

D. S. STEWART
University of Illinois
Urbana, Illinois, IL 61801

Since during the Symposium I have been repeatedly asked by various friends and colleagues about the differences between the WBL model and DSD, I thought that I should make a comment. The WBL model referred to is exactly the same as the DSD method. Indeed it should be pointed out that in the summer of 1987 I spent six weeks visiting Prof. John Clarke of the Cranfield Institute of Technology, UK, where I worked on various aspects of DSD, a theory that John Bdzil and I had been developing together. My stay at Cranfield was supported by funds from AWE, Aldermaston. During my stay at Cranfield a briefing at Aldermaston was given by myself to Aldermaston staff, which included B Lambourn. Indeed copies of a joint talk that John and I had prepared was provided and later a technical report, Stewart D.S. "Detonation Shock Dynamics", Cranfield Co A Report No NFP/8707, August 1987, for Aldermaston Contract No NNS/32A/1A91965, was written before my departure from Cranfield. Later this same report appeared as Stewart D.S. and Bdzil J.B. "A Lecture on Detonation Shock Dynamics", Mathematical Modelling in Combustion Science, Lecture Notes in Physics, 299, p17, 1988. The paper and talk described all the main elements of DSS (sic), sonic eigenvalue detonation, intrinsic co-ordinates, intrinsic evolution equations, angle confinement boundary conditions, initial detonation curvature and the possibility of dead zones and extinction. In the last (not the current) detonation symposium the WBL method was presented by some of the present authors and there was an omission of reference to our earlier paper and acknowledgement of the Cranfield report and briefing at Aldermaston

REPLY BY D. C. SWIFT

Depending on what is meant by "model" or "method", whilst similar, DSD and WBL are not exactly the same in derivation, history or algorithms. The name "WBL" is historical, based on the perceptions of those contributing to the work in the particular group responsible for these developments at Aldermaston.

The authors of the present paper have neither seen nor referred to the works cited.

In our opinion, this is more an example of parallel and convergent development, with interaction between groups at AWE and LANL. From an AWE perspective, the WBL model is based significantly on inclusive work dating back to the 1960s.

This paper is a report on the application of the WBL model to two explosives – for original references please refer to "Application of Whitham's Shock Dynamics Theory to the Propagation of Divergent Detonation Waves", B. D. Lambourn & D. C. Swift, in the 9th Detonation Symposium..